



SYNTHESIS AND CHARACTERIZATION OF $(\text{NH}_4)_2\text{MnMg}(\text{SO}_4)_2 \cdot 6\text{H}_2\text{O}$

Binitha S.D

Department of Chemistry, Christian College Kattakada, Kerala, India.

Abstract

*New mixed crystals of the Tutton's salt family with chemical formula $(\text{NH}_4)\text{Mn}_{0.5}\text{Mg}_{0.5}(\text{SO}_4)_2 \cdot 6\text{H}_2\text{O}$ were grown by employing slow evaporation solution growth technique. The coexistence of manganese and magnesium ions in the mixed crystal were characterized by X-ray diffraction (XRD) and Fourier Transform Infrared (FT-IR) spectroscopy. This type of material has been studied extensively due to its various potential technological applications. The crystal structure had been confirmed by XRD and the study confirmed that ammonium manganese magnesium sulfate hexahydrate (AMMSH) crystal belongs to monoclinic space group $P2_1/a$. FTIR spectral analysis were done to study the vibrational bands of AMMSH crystal and assigned the modes of vibration to different functional groups. In addition, antibacterial activity of the crystal was analyzed using agar well-diffusion method. The antibacterial activity of methanol and aqueous extracts of AMMSH were investigated against elected human pathogens such as *Escherichia coli*(gram-negative) and *Streptococcus sp* (gram-positive). Results confirmed that, the gram-positive strain is found to be more sensitive than the gram-negative strain with excellent and long-term antibacterial activity.*

Keywords:*Ammonium Manganese Magnesium Sulfate Hexahydrate; Characterisation; X-Ray Diffraction; Fourier Transform Infrared; Antibacterial Activity.*

Introduction

Recently our scientific interest and efforts have been concentrated in the study on growth and characterization of Tutton's salt due to its potential technological applications such as chemical energy storage, ultraviolet (UV) light filters [1, 2], UV made sensors, spaceships, solar energy absorber and even in missile approach warning systems. The crystals of Tutton's salt are used to locate and track the sources of ultraviolet energy [3] and sometimes they are used to block UV radiation. Tutton's salt doped with rare earth ions are of particular interest for optical applications, such as solid-state lasers [4-7]. Most recently, Tutton's salts acts as promising materials for applications as ion-conductors in batteries, electrodes, cathodes, solid electrolytes and even in lithium or sodium batteries [8]. The family of Tutton's salt is a group of isomorphous compounds with the chemical formula $A_2B(\text{XO}_4)_2 \cdot 6\text{H}_2\text{O}$ where $A = \text{K}, \text{NH}_4, \text{Rb}, \text{Cs}, \text{Tl}$; $B = \text{Mg}, \text{Mn}, \text{Fe}, \text{Co}, \text{Ni}, \text{Cu}, \text{Zn}, \text{Cd}, \text{V}, \text{Cr}$; $X = \text{S}$ or Se . The crystallographic structure of the Tutton's salt belongs to the monoclinic space group $P2_1/c$ [$Z = 2$] [9, 10]. This crystal contains two octahedral hexahydrate complexes $[\text{M}'(\text{H}_2\text{O})_6]^{2+}$ in the crystal unit cell, Where M' is a bivalent cation and M is a monovalent cation.

The crystal structure of magnesium ammonium sulfate hexahydrate [11] investigation has been reported. There are some studies about the Manganese sulfates such as potassium manganese nickel sulfate hexahydrate [12, 13], potassium zinc manganese sulfate [14] and so on. Recently Ramaswamy et al has carried out a study based on growth, structure and characterization of Potassium magnesium manganese sulfate hydrate [15]. Metal-based complexes have significant antibacterial, anticancer and antiviral effects [16]. Infectious diseases are the leading cause of death worldwide. Antibiotic resistance has become a global concern. The clinical efficacy of many existing antibiotics is being threatened by emergence of multi drug resistant pathogens. In the past decades, plenty of people have suffered from



diseases caused by unsafe drinking water and food containing bacteria such as *Escherichia coli*, *Staphylococcus aureus* and *Bacillus subtilis*. The traditional low molecular weight antibacterial materials have many disadvantages, such as toxicity to the environment and short-term antibacterial activity. Hence, there is an urgent need for the development of effective antibacterial materials [17].

Although extensive studies have been carried out on Tutton's salts, the growth, characterization and structure of $(\text{NH}_4)\text{Mg}_x\text{Mn}_{(1-x)}(\text{SO}_4)_2 \cdot 6\text{H}_2\text{O}$ mixed crystals have not been reported so far. The aim of this paper is to carry out a crystal-chemical and antibacterial study of the synthetic compounds of general chemical formula $(\text{NH}_4)\text{Mn}_x\text{Mg}_{(1-x)}(\text{SO}_4)_2 \cdot 6\text{H}_2\text{O}$. In this work, the hexahydrate crystals of magnesium and manganese ammonium sulfate were synthesized by slow evaporation solution growth technique. These crystals were characterized by XRD and FT-IR. Further, antibacterial study was carried out by agar-well diffusion method with two human pathogens *Escherichia coli* (gram-negative) and *Streptococcus* sp (gram-positive) in comparison with a commercially available antibiotic, Amoxycillin.

Materials and Methods

Synthesis

Pure AMMS was prepared by mixing equimolar concentrations of $(\text{NH}_4)_2\text{Mg}(\text{SO}_4)_2 \cdot 6\text{H}_2\text{O}$ and MnSO_4 using deionized water as a solvent by the slow evaporation technique. All starting materials used were highly pure. Colored crystals appeared after about 7 days under the experimental conditions. The resulting crystals are recovered from the solution by filtration and washing with an organic solvent and then drying in air. The crystals were finely ground. The powder were ground in an agate mortar and then pressed to 6 MPa into cylindrical pellets. The pellets were then sintered in air for 7 hour. Good quality crystals were harvested after 15 days. Photograph of mixed crystals is shown in Fig. 1.



Fig.1 Image of AMMSH crystal

Characterization

XRD measurements were performed to analyze the crystalline structure of monocrystals using the Rigaku MiniFlex 600 X-ray diffractometer. The radiation used was CuK with wavelength, $\lambda = 1.5406 \text{ \AA}$ and energy, $E = 8.04 \text{ keV}$ at room temperature. Samples selected for these measurements needed to



be approximately 0.1 mm in size, so that they can be attached to the goniometer of the equipment and completely bathed by the X-ray beam. The measurements were swapped from $2\theta = 10^\circ$ to 80° with the step of 0.06° , copper target at 40kV, 30mA, and a scanning speed of $0.06^\circ/\text{min}$ and incident wavelength $\lambda = 1.5406\text{\AA}$. A Perkin Elmer Fourier transform infrared spectrometer was used to record the FTIR spectra in the range $500\text{--}4500\text{cm}^{-1}$ by the KBr pellet method to study the functional groups of AMMSH crystal.

The antibacterial screening was determined using agar-well diffusion method. The methanolic and aqueous extracts of AMMSH were prepared by dissolving 100mg fine powder separately in 1 ml of methanol and water respectively. The contents were kept in shaker for 24 h (stock concentration of the extract: 100mg/mL). After 24 hours, the supernatant was filtered and used for the study. From the stock concentration (100 mg/mL), a lower concentration of 50 mg/mL was prepared. The inoculum of *Escherichia coli* and *Streptococcus* sp., were prepared in nutrient broth medium and kept incubation at 37°C for 8 hours. After growth was observed, the cultures are stored in the refrigerator at $2\text{--}8^\circ\text{C}$ for analysis. 20 ml of sterilized Muller Hinton Agar was poured into sterile petriplate, after solidification, $100\ \mu\text{l}$ (10^5c.f.u./mL) of test organism were swabbed on the respective plates. Wells of 6 mm diameter were punched into the agar medium and filled with $100\ \mu\text{L}$ of plant extract (of 100 mg/mL and 50 mg/mL concentration), antibiotic solution (positive control) and solvent blank (methanol and water) (negative control). The plates were incubated for 24 hours at 37°C . After incubation the diameter of inhibitory zones formed around each discs were measured in cm and recorded.

Results

The crystalline structure and crystallographic orientation of prepared sample was investigated by XRD measurements. Good monocrystal with natural and well-developed faces were obtained throughout the composition range. Fig. 2 shows the X-ray diffraction patterns of triple salt $(\text{NH}_4)_2\text{Mn}_{0.5}\text{Mg}_{0.5}(\text{SO}_4)_2 \cdot 6\text{H}_2\text{O}$. The strongest peaks observed were found at $2\theta = 21.54^\circ, 29.29^\circ, 40.91^\circ, 43.20^\circ, 52.89^\circ, 57.80^\circ, 67.1^\circ$ and 74.58° related to the planes having miller indices (201), (200), (211), (301), (321), (411), (332), (310) and (502) respectively corresponding to lattice parameters $a = 5.340\text{\AA}$, $b = 9.524\text{\AA}$, $c = 10.235\text{\AA}$ and $\alpha = 90^\circ$, $\beta = 100.070^\circ$, $\gamma = 90^\circ$. The cell parameters were in fine conformity with the reported values [15].

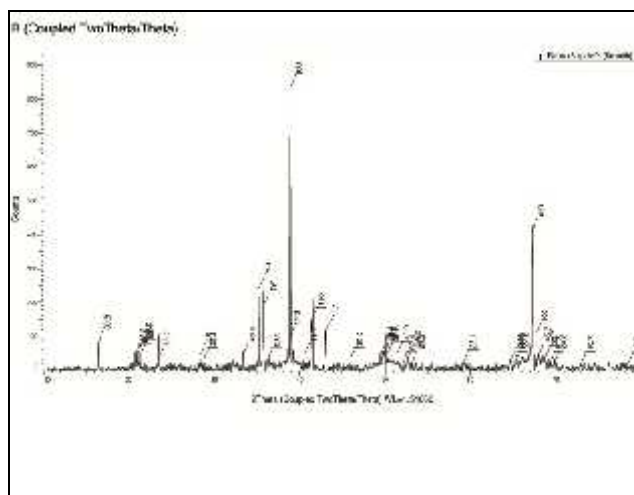


Fig. 2 XRD pattern of AMMSH



Fourier transform infrared spectroscopy was used for the identification of functional groups in the synthesized crystals. The spectrum was recorded in the spectral range of 500-4500 cm^{-1} shown in Fig. 3.

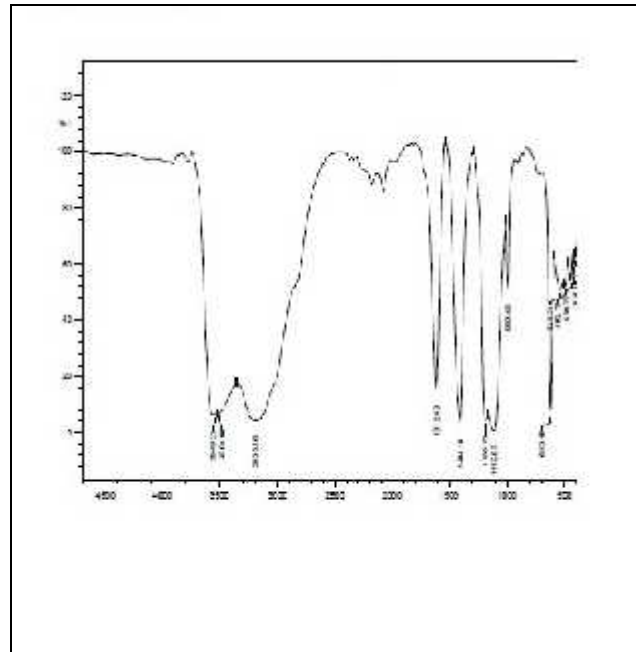


Fig. 3 FT-IR spectrum of AMMSH

Agar-well diffusion method was used to investigate the antibacterial activity of methanol and aqueous extracts of AMMSH against selected human pathogens such as *Escherichia coli* and *Streptococcus* sp and the results were shown in Tables 1 and 2. These two different pathogens have also tested with commercially available antibiotic (Amoxycillin) and results were indicated in Table 3. The antibacterial activity of methanolic and aqueous extracts of AMMSH and standard antibiotic amoxycillin using agar well-diffusion method is shown in Fig. 4.



Fig. 4 Antibacterial activity of methanolic (A) and aqueous extracts (B) of AMMSH and standard antibiotic amoxycillin using agar well-diffusion method

Discussion

XRD

XRD measurements reveals that the crystal belongs to monoclinic system with centrosymmetric space group $P2_1/c$ and the cell parameters are $a = 5.340 \text{ \AA}$, $b = 9.524 \text{ \AA}$, $c = 10.235 \text{ \AA}$, $\alpha = \beta = \gamma = 90^\circ$, $V = 520.533 \text{ \AA}^3$ and $Z = 2$. The well defined Bragg's peaks at specific 2θ angles show good



crystallinity of the materials. The multiple peaks with large value of full width at half maximum indicates that the specimen contains many mosaic blocks which are disoriented to each other with their adjacent regions as observed in benzimidazole single crystals grown by vertical Bridgman technique [18]. Impurities present in the raw material and thermal or mechanical fluctuations during the growth process may be responsible for such features of diffraction curve. The refinement of the single crystal depicts that the crystalline size was calculated by using Debye Scherrer equation,

$$\tau = \frac{K\lambda}{\beta \cos \theta}$$

The crystalline size of prepared crystal was found to be 14 nm corresponding to the (301) plane. Thus, the crystallographic data had a good approximation with the experimental diffraction.

FT-IR spectroscopy

In FT-IR spectrum, the peak at 3504.00 cm⁻¹ is attributed to the free OH stretching. The strong intensity peak at 1612.40 cm⁻¹ explains the OH group confirmation [19]. A strong vibration band around $\nu_2 = 1622.13$ cm⁻¹ is due to the in-plane bending vibration of water molecules caused by the rocking and scissoring of hydrogen atoms. The observation of bands in the spectral region of 1700-1400 cm⁻¹ shows water being strongly hydrogen bonded in the crystal structure with different molecular bonds. The NH₄⁺ tetrahedra present a very strong band at $\nu_4 = 1404.18$ cm⁻¹ corresponding to the N-H bending mode. The SO₄²⁻ tetrahedra presents a strong peak at $\nu_3 = 1112.93$ cm⁻¹ corresponding to the triply degenerated asymmetric stretching mode and a very strong peak at $\nu_4 = 630.25$ cm⁻¹ corresponding to the triply degenerated bending mode [15]. The FTIR spectrum of AMMSH confirms that the grown crystal forms a combination of monomeric crystals.

Antibacterial activity

Methanol and aqueous extracts of AMMSH used against the pathogenic organisms have showed varied degree of antimicrobial activity against the pathogens in agar-well diffusion method.

Antibacterial susceptibility testing of methanolic extract of AMMSH: The two concentrations of the extract were found to be effective against the selected strains (*Streptococcus* and *E.coli*). The growth of these organisms was inhibited by the extracts forming an inhibitory zone of different diameters. The highest inhibition was observed with *Streptococcus*, which was found to be 2.4 cm at 100mg/ml concentration. Similarly, a good inhibitory zone (2.2 cm) was also observed with *E.coli* at 100mg/ml concentration. These results revealed the significant antibacterial activity of the extract against studied bacteria.

Antibacterial susceptibility testing of aqueous extract of AMMSH: The highest inhibition was observed with *Streptococcus*, which was found to be 2 cm at 100mg/ml concentration. Similarly, a satisfactory inhibitory zone (1.9 cm) was also observed with *E.coli* at 100mg/ml concentration. These results confirmed the significant antibacterial activity of the extract against studied bacteria. In this study, the highest concentration of the extract (100mg/ml) showed the highest activity than the rest [16]. The preliminary screening for antimicrobial activity showed, that the methanolic extract of AMMSH exhibited maximum inhibitory zone (2.4 cm) against *Streptococcus* sp. and for *E.coli* a satisfactory zone of 2.2cm. While the aqueous extracts of AMMSH showed least inhibition when compared with methanol activity. In addition, it is clear from the results that, the gram-positive strain (*Streptococcus*) is found to be more sensitive than the gram-negative strain (*E.coli*). Because its zone of inhibition is



higher than that of *E.coli*. Therefore, AMMSH has potential applications as a broad-spectrum antibacterial agent.

Conclusion

The AMMSH crystal has been synthesized by slow evaporation growth technique and pure crystals with good crystallinity were obtained. The resultant crystal showed characteristic morphology of the Tutton's salts with empirical formula $(\text{NH}_4)\text{Mn}_{0.5}\text{Mg}_{0.5}(\text{SO}_4)_2 \cdot 6\text{H}_2\text{O}$ and has been put under successive investigations to study their structural properties. . The crystalline structure and crystallographic orientation of as-prepared samples were investigated by XRD measurements. The refinement of the diffraction pattern revealed that the crystal has monoclinic crystal system with space group $\text{P}2_1/\text{c}$. FTIR spectrum of AMMSH identified the functional groups present in it. The vibrational modes of octahedral complexes, NH_4^+ and SO_4^{2-} tetrahedra are obtained from FTIR. AMMSH crystal was assayed for its antibacterial activity and results obtained gives a scope for future pharmacological applications in designing better and more active drugs.

Acknowledgements

The author is thankful to Department of Chemistry Christian College Kattakada for providing facilities to do the research work.

References

1. Qian X, Liu H (2011) Crystals $\text{M}_2\text{Ni}(\text{SO}_4)_2 \cdot \text{XH}_2\text{O}$ ($\text{M} = \text{Na}$, $\text{X} = 4$; $\text{M} = \text{K}$, NH_4 , Rb , Cs , $\text{X} = 6$): Crystal Structures, Spectrum and Thermal Stability Characterizations. *Adv Mater Res* 332-334:1687-1690. <https://doi.org/10.4028/www.scientific.net/AMR.332-334.1687>
2. Manomenova VL, Rudneva EB, Voloshin AE (2016) Crystals of the simple and complex nickel and cobalt sulfates as optical fibres for the solar-blind technology. *Russian Chem Rev* 85:585. <https://doi.org/10.1070/RCR4530>
3. Singh NB, Partlow WD, Strauch S, Stewart AM, Jacovitz JF, Coffey DW, Mazelsky R, Smith JDB (1998) Crystals for ultraviolet light filters. Google Patents.
4. Soumati A, Martin IR, Zayani L, Hernandez-Rodriguez MA, Soler-Carracedo K, Lozano-Gorrin AD, Lalla E, Chehimi DBH (2016) Synthesis, characterization and spectroscopic properties of a new Nd^{3+} -doped Co-picromerite-type Tutton salt. *J Lumin.* 177:93-98. <https://doi.org/10.1016/j.jlumin.2016.04.033>
5. Soumati A, Zayani L, Palomino JM, Cruz-Yusta M, Vicente CP, Hassen-Chehimi DB (2015) Synthesis, characterization and thermal analysis of $\text{K}_2\text{M}(\text{SO}_4)_2 \cdot 6\text{H}_2\text{O}$ ($\text{M} = \text{Mg}$, Co , Cu). *J Therm Anal Calorim.* 122:929-936. <https://doi.org/10.1007/s10973-015-4779-6>
6. Soumati A, Martin IR, Zayani L, Lozano-Gorrin AD, Ben Hassen Chehimi D (2017) Luminescence properties of Pr^{3+} ion doped Mg-picromerite Tutton salt. *J Lumin.* 188:148-153. <https://doi.org/10.1016/j.jlumin.2017.04.022>
7. Soumati A, Martin IR, Zayani L, Hernandez-Rodriguez MA, Soler-Carracedo K, Lozano-Gorrin AD, Ben Hassen Chehimi D (2016) Blue up-conversion emission of Yb^{3+} -doped langbeinite salts. *Opt Mater.* 53:190-194. <https://doi.org/10.1016/j.optmat.2016.01.052>
8. Bejaoui A, Souamti A, Kahlaoui M, Lozano-Gorrin AD, Morales Palomino J, Ben Hassen Chehimi D (2019) Synthesis, characterization, thermal analysis and electrical properties of $(\text{NH}_4)_2\text{M}(\text{SO}_4)_2 \cdot 6\text{H}_2\text{O}$ ($\text{M} = \text{Cu}$, Co , Ni). *Mater Sci Eng B.* 240:97-105. <https://doi.org/10.1016/j.mseb.2019.01.016>



9. Margulis TN, Templeton DH (1962) Crystal structure and hydrogen bonding of magnesium ammonium sulfate hexahydrate. *Z Kristallogr Cryst Mater.* Bd. 117:344-357.
10. Montgomery H, Lingafelter EC(1964) The crystal structure of Tutton’s salts. II. Magnesium ammonium sulfate hexahydrate and nickel ammonium sulfate hexahydrate. *Acta Crystallogr A.* 17:1478-1479.
11. Ramaswamy G, Bhagavannarayana G, Madhurambal G, Meenakshisundaram S(2012) Crystal growth, structure, crystalline perfection and characterization of zinc magnesium ammonium sulfate hexahydrate mixed crystals $Zn_xMg_{(1-x)}(NH_4)_2(SO_4)_2 \cdot 6H_2O$. *J. Cryst. Growth.* 352:137-142. <https://doi.org/10.1016/j.jcrysgro.2012.02.028>
12. Duraikkan V, Bahadur SA, Athimoolam S (2012) Crystal growth and characterization of potassium manganese nickel sulfate hexahydrate – a new UV filter. *J Miner Mater Charact Eng.* 11:1121-1125. doi:10.4236/jmmce.2012.1111120
13. Masilamani V, Shanthi J, Sheelarani V (2014) Growth and analysis of NSH and KMSNH crystals by slow evaporation technique. *Crystallogr Rep.* 59:1114-1117. <https://doi.org/10.1134/S1063774514070141>
14. Vijila Manonmani J, Bhagavannarayana G, Ramasamy G, Subbiah Meenakshisundaram, Amutha M (2014) Growth, structure and spectral studies of a novel mixed crystal potassium zinc manganese sulfate. *Spectrochim Acta A.* 117:9-12. <https://doi.org/10.1016/j.saa.2013.07.089>
15. Ramasamy G, Anandakumaran J (2020) Crystal, growth, structure and characterization of Tutton’s salt mixed crystals-Potassium magnesium manganese sulfate hexahydrate. *Int J Pharm Res Chem.* 10(1):54-62. DOI: [https://dx.doi.org/10.33289/IJRPC.10.1.2020.10\(12\)](https://dx.doi.org/10.33289/IJRPC.10.1.2020.10(12))
16. Sagunthala P, Veeravazhuthi V, Yasothea P, Hemalatha P (2016) Growth, characterization, antimicrobial and anticancer activities of L alanine added Nickel sulfate crystals. *World J Pharm Res.* 5(8):414-425. doi: 10.20959/wjpr20168-6738
17. Qingguo Meng, Lintong Wang, Dongfang Wang, Jianjian Yang, Chen Yue, Jitao Lu (2017) Synthesis, Crystal Structure, Photoluminescence Properties and Antibacterial Activity of a Zn(II) Coordination Polymer Based on a Paddle-Wheel Cluster. *Crystals.* 7:112-119. <https://doi.org/10.3390/cryst7040112>
18. Vijayn N, Bhagavannarayana G, Ramesh Babu R, Gopalakrishnan R, Maurya KK, Ramasamy P (2006) A comparative Study on Solution- and Bridgman-Grown Single Crystals of Benzimidazole by High-Resolution X-ray Diffractometry, Fourier Transform Infrared, Microhardness, Laser Damage Threshold, and Second-Harmonic Generation Measurements. *Cryst Growth Des.* 6:1542-1546. doi: 10.1021/cg060002g
19. Nakamoto K (1986) Raman Infrared spectra of inorganic coordination compounds. Wiley. New York, pp 242-244

Table 1: Antibacterial activity of different concentrations (100mg/ml and 50mg/ml) of methanolic extracts of AMMSH by agar well-diffusion method.

Sl.No	Organism	Concentration of the extract	Resistant	Sensitive	Zone diameter (in cm)
1.	<i>Escherichia coli</i>	100mg/ml		+	2.2
		50mg/ml		+	1.6
2.	<i>Streptococcus sp.</i>	100mg/ml		+	2.4
		50mg/ml		+	1.7



Table 2: Antibacterial activity of different concentrations (100mg/ml and 50mg/ml) of aqueous extracts of AMMSHby agar well-diffusion method.

Sl.No	Organism	Concentration of the extract	Resistant	Sensitive	Zone diameter (in cm)
1.	<i>Escherichia coli</i>	100mg/ml		+	1.9
		50mg/ml		+	1.4
2.	<i>Streptococcus sp.</i>	100mg/ml		+	2.0
		50mg/ml		+	1.5

Table 3: Antimicrobial activity of standard antibiotic (Amoxycillin)

Organism	Zone diameter of amoxycillin
<i>E.coli</i>	3.5
<i>Streptococcus sp.</i>	3.1